

MRI MICROCOILS FOR IMAGING INDIVIDUAL CELLS

Matthew Feldman,* Michael Lanagan,# and Steven Perini⁺

Department of Electrical Engineering
The Pennsylvania State University, University Park, PA 16802

*Undergraduate Student of
Department of Electrical & Computer Engineering
University of Florida
Gainesville, FL 32612

ABSTRACT

With high-magnetic-field MRI scanners, it becomes necessary to finely tune the impedance and resonating frequency of a receive-coil electronically. B₁-producing coils for large magnets, especially those that target 600 MHz or greater, are extremely sensitive to external influences and coupling with the copper shielding, metal inside the machine, and the sample being imaged. Signal-to-noise ratio and resolution can be sharply increased if the resonant frequency of the coil can be tuned simultaneously while all of these factors have been introduced, rather than by trial-and-error by taking apart the set up each time to make an adjustment.

Varactors are voltage tunable capacitors that are a potential option for allowing the user to tune the coil electronically from a distance. This study has shown that they are capable of tuning a circuit to a desired frequency, as viewed from the S₁₁ parameter on a Vector Network Analyzer. However, the Q-factor of hyperabrupt-junction varactors is so low that the S₂₁ does not show any discernable peak. Therefore, this method of tuning is not the most desirable for high-frequency applications, as loss is directly related to frequency.

A Helmholtz coil proved to be a valuable design for creating a uniform magnetic field. Though the dimensions of the setup in this study were not ideal, they seemed to indicate that a properly designed coil will exhibit rewarding behavior. The magnetic field passing through the midplane seemed to be very uniform, except for where there was a deliberately-placed gap in the coil for design purposes. The behavior of the magnetic field along the axis passing through the centers of the two loops was inconclusive with the results from this

Primary Faculty Mentor

⁺ Secondary Faculty Mentor

study, but further experimentation can be done with existing prototypes to assess this.

It would be advantageous to assess whether it is the complication of the circuit with a varactor setup or the varactors themselves that are interfering with the emission of signal. Numerous steps can be taken in the future, including using alternative electronic tuning methods or using different components to test specific parts of the circuit, in order to improve the SNR and resolution. In the future, these coils can be used to advance biological knowledge of tissue structures and real-time understanding of flow, diffusion, and perfusion of substances.

INTRODUCTION

Magnetic Resonance

The goal of this project is to use the nuclear magnetic resonance (NMR) signal to obtain images of individual biological cells. In NMR imaging, magnetic fields induce atoms with non-zero nuclear spin to give off radio frequency (RF) signal. Specifically, a B_0 magnetic field aligns the net nuclear spin of hydrogen atoms within substances such as adipose and water. A B_1 field is then used to cause these spins to precess at a “Larmor” frequency. This frequency is determined by both the gyromagnetic ratio of the atom and the value of B_0 . Three orthogonal gradient coils are used to select a slice and cause a position-based alteration of frequency and phase that can be used to discern voxels in an image. The B_1 process involves both transmission in the form of an RF electromagnetic wave in the shape of a sinc function and the reception of the RF signal emitted by the nuclear spins using Faraday’s Law. All of these various coils, except for B_1 receive, are fully contained within the 14-T MRI scanner that is to be used in this project. However, the receive coil must be custom built.

In recent years, some companies have already built coils that can be used to image small objects, but the signal-to-noise ratio and resolution of these images are less than desirable to biologists and researchers.¹ The signal-to-noise ratio can be improved by using a stronger B_0 field, improving the sensitivity of the receive coil, and lengthening the imaging sequence. The density of k -space, field of view, and slice thickness determines the spatial resolution. The coil built in this project is designed to improve these parameters.

Helmholtz Coils

The coil design used in this resonator is a Helmholtz coil. This coil design consists of two loops of equal radius separated by some distance, as shown in Figure 1. When the distance between them is equal to their radius, the magnetic field is strong and uniform. It is a volume coil, which makes it better than a surface coil, considering its field strength and uniformity. This is ideal for preventing artifact. The magnetic field, as a function of the distance from the midplane, r , is given by:

$$B(r) = I \times 10^{-7} \int_0^{2\pi} \frac{2a(a - r\cos(\theta))d\theta}{(a^2 + b^2 + r^2 - 2ar\cos(\theta))^{\frac{3}{2}}}$$

where I is the current through the coils, a is the radius of the coils, and b is the distance between them. By changing the values of parameters in this equation, it is possible to get various field strength designs. If the distance between the coils is too small, there will be strong magnetic field when r is close to a and weak magnetic field when r is close to zero. If the distance between the coils is too large, the magnetic field will peak in when r is close to zero, rather than creating a plateau across all values of r . Water phantoms can be used to assess the uniformity of the magnetic field in an MRI scanner.

Tunability

Since the inductance of the coil is fixed, a capacitor in parallel must be adjusted to tune the resonant frequency of the circuit, while a capacitor in series must be adjusted to tune the impedance of the circuit. Mechanically tunable capacitors have a high quality (Q) factor and are the most straightforward way of achieving tunability, but are impractical because the coil circuit is inserted deep in the imaging coil and inaccessible during the imaging sequence. Therefore, a digital means of tuning must be used. This project attempts to use varactor diodes to tune these two capacitances. These components vary capacitance with potential difference introduced across them. Therefore, cables can be fed through the MRI tube and out of the room, where DC power supplies can be used to supply the potential differences across both varactors. The junction capacitance, C_j , of a varactor as a function of reverse bias voltage, V_r , can be determined by the equation:

$$C_j(V_r) = \frac{C_{j0}}{\left(1 + \frac{V_r}{\Phi}\right)^\gamma}$$

where γ is a constant (equal to 0.5 for hyperabrupt junction and greater than 0.5 for abrupt junction varactors) and Φ is contact potential (about 0.75 for Si). The type of junction refers to the way the varactor was processed. Silicon and Gallium Arsenide are the only two materials a varactor can be made of.

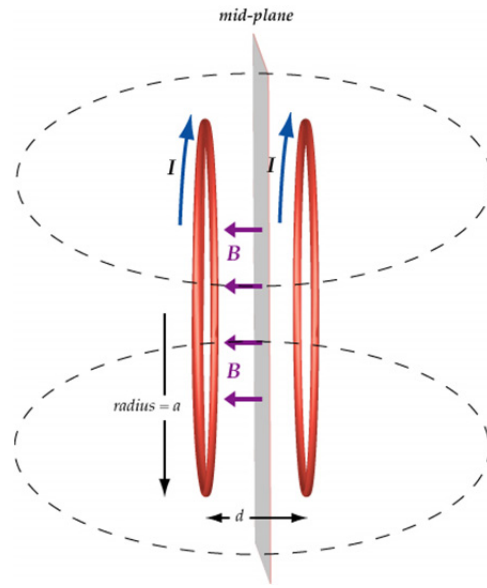


Figure 1: The variables that determine the uniformity of a magnetic field caused by a Helmholtz pair are the radius of the coils and the distance between them

EXPERIMENT DESCRIPTION

Equipment

A vector network analyzer (VNA) made it possible to see where the coil was resonating and how sharp the peak was. This piece of equipment is capable of testing a device at a range of frequencies in the microwave range and returning various data of interest. Specifically, the VNA was used to determine the S_{11} and S_{21} parameters of the chip. These parameters are ratios and measured in decibels. S_{11} represents the ratio of the signal being introduced into the chip through the 50- Ω coaxial cable to the signal being returned back through the coax. A loop antenna was used as a load to obtain S_{21} , which represents the ratio from signal introduced through port 1 (the coil) to signal received through this antenna (port 2). The VNA also has a Smith Chart feature, which can be used to see whether the value of impedance of the circuit and whether it is inductive, capacitive, or resistive. This is helpful in determining if a peak in the frequency-versus-dB chart is actually a resonance frequency or a coincidental reflection of waves.

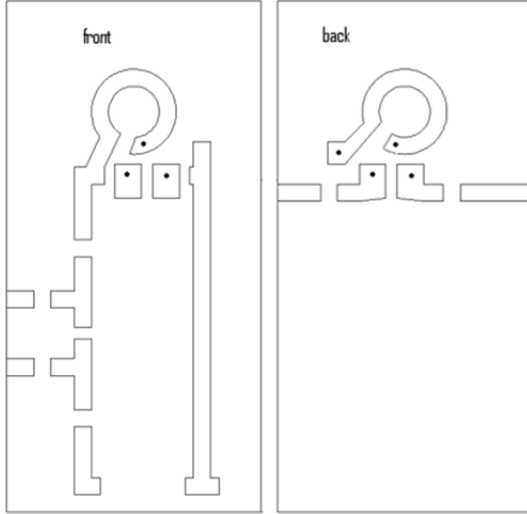


Figure 2: Actual layout for chip, with gaps for components and dots for through-connections

Proof of Concept

The feasibility of varactors was tested in many different steps. Due to cost restraints, magnetic varactors were used in the early models. The varactor requires two capacitors, two resistors, and biasing lines in order to operate, as shown in Figures 2 and 3. A DC reverse bias across the varactor is what changes its capacitance. Two large resistors must be placed in the DC circuit so that there is little current running across the varactor, and the actual signal going through the coil's circuit is not affected. Two large capacitors must isolate the DC circuit so that the potential difference is applied across only the varactor of interest and not the rest of the circuit. Using large isolating capacitors ensures that relatively small varactor capacitances dominate the equivalent capacitance. Two possible pitfalls with varactor tuning are that varactors are relatively lossy, and

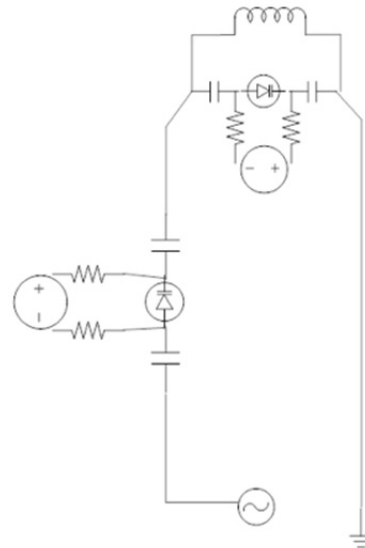


Figure 3: Schematic circuit diagram of 600-MHz resonator.

integrating them into a small chip may overcomplicate the circuit and cause incidental capacitance and inductance in the traces, as can be seen in Figures 2 and 3. Also, the varactors have a range of just a few picofarads. This means that the values of the isolating capacitors must be chosen carefully to allow the equivalent capacitance to be the necessary amount.

A CO₂ laser was used to cut out an AutoCAD-drawn copper trace design onto a 30 mm × 15 mm piece of Roger RO3000. This material is a ceramic and woven glass substrate with very low dielectric loss, and was used because high permittivity ceramic dielectrics can potentially ameliorate some of the challenges of high frequency coil design and encourage strong magnetic fields in a compact design.² The excess copper was chemically etched off, leaving a ceramic a sturdy platform for soldering pieces on and off. With this board, the experimental components were attached to get a sense of the frequency range with certain values of capacitance. An SMA connector was used to connect to the waveguide port.

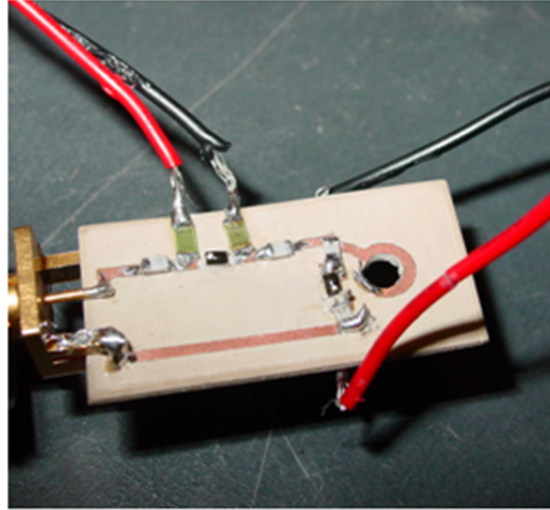


Figure 4: Photograph of finished product.

After this initial test, nonmagnetic components were used. The nonmagnetic varactors are hyper-abrupt junction, which means they have a lower Q . This final product can be seen in Figure 4. Note that the varactors were attached using silver paint, rather than solder, due to a coating that quickly wore off the varactors, preventing them from bonding to solder. The final step of the process is to drill a hole in the Helmholtz coil and grow cells. Once this is done, the coil is to be mounted on an MRI probe and inserted into the scanning machine. Once the coil is in the machine, the presence of new materials and a large magnetic field will make the tuning process more complicated than it is in a lab. The circuit must be out of tune while the MRI machine undergoes its B_1 transmission process, but tuned quickly after in order to receive the signal. Various switches may be used to achieve this rapid tuning.

CST Microwave Studio was used to design a model of the coil and test the magnetic field uniformity and viability of the created circuit. MathCAD was used to mathematically calculate the theoretical distribution of the magnetic field in a coil, given our dimensions.

EXPERIMENT RESULTS

Theoretical Models

According to the CST Microwave Studio model of the circuit, it was possible

for our circuit to resonate at 600 MHz, given its geometry. The magnetic field within the Helmholtz coil clearly indicated that the field strength was somewhat hourglass shaped. There were a few limitations with CST in predicting what the circuit would look like. Firstly, there are no preset capacitors or varactors in the program. Therefore, having a specific gap in the copper trace set capacitance values. In the physical prototype, the ceramic capacitors and varactors actually have their own loss and inductance associated with their geometry. CST also did not allow for resistors or biasing lines to be added to the circuit. Had this been possible, it may have been possible to see if there is any coupling between the additional traces added to allow biasing lines.

After the chip was fabricated, the exact dimensions were input into a MathCAD file to calculate what the magnetic field should look like. The graph, Figure 5, showed that there is a noticeable dip in the midway between the coils. The ideal geometry would yield a nearly perfectly uniform magnetic field. When the imperfect coil is used in an MRI scanner, this deformity should be manifested as the middle of the image being darker than the ends of the image.

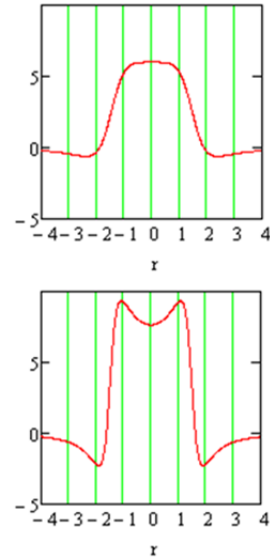


Figure 5: Magnetic field caused by Helmholtz coil with 1.5-mm radius. The top image represents magnetic field as a function of distance from the midplane if the separation between the two coils is ideal (1.5 mm). The bottom image represents the actual separation of the Helmholtz coil used in this study, 0.75 mm.

Physical Results

After the coil was constructed with varactor setups and was tuned to 600 MHz, data from the VNA were recorded with a LabVIEW data acquisition program. According to S_{11} , the varactors were a viable method of tuning the circuit. The impedance was able to be matched at 50Ω when the resonant frequency of the system was 600 MHz.

However, looking deeper into the setup and measuring S_{21} , the

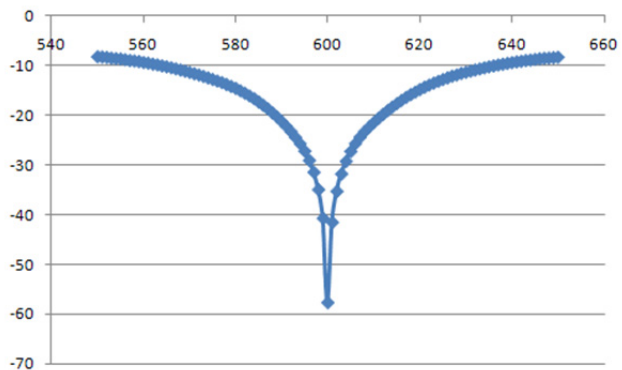


Figure 6: Plot of S_{11} versus frequency, when varactors are used to tune the circuit to 600 MHz.

varactors proved to be far too lossy for MRI applications. When a loop antenna was brought close to the coil, there was no discernable peak in the S_{21} logarithmic magnitude (Figure 7). This means that although the circuit was resonating at 600 MHz and very little signal was reflected back into port 1, very little signal was actually emitted as RF through the coil. It is believed that the low Q value of the varactors is the reason for this loss in energy. They may be absorbing most of what would normally be emitted.

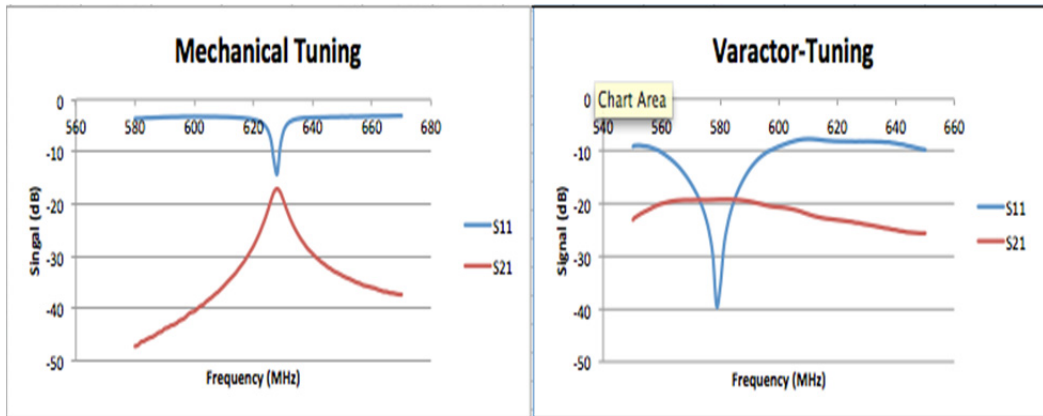


Figure 7: S_{11} and S_{21} comparison between the varactor-tuning and mechanical-tuning. The bandwidth of S_{21} for the mechanical setup has a much smaller bandwidth.

Unfortunately, when the chip was mounted on a 14-T MRI probe connected to the VNA with a BNC cable, it was impossible to recreate the S_{11} peak. Jarring the DC bias wires had a major impact on the S_{11} chart. It is unclear why this happened, as there should not be much coupling happening with the introduction of DC to the chip. A possible solution would be to use solid wire rather than bundled wire to connect to the power supply.

The S_{21} graphs shown in Figure 7 have implications from the perspective of MRI scans. When these particular coils are placed in the MRI scanners, the S_{11} parameter will be used to tune them, but S_{21} indicates of how well they will receive signal. Since these are receive-only coils, their function is to resonate under an induced oscillating *emf*, as per Faraday's Law, caused by T_2 precession of magnetic spin in the target substance. This whole process is the reverse of the S_{21} parameter, which makes it a good indication of how well the coil will operate. If the coil can emit RF energy at a certain frequency, it is also capable of picking up signal at that same frequency. When a varactor-tuned circuit is tested in an MRI scanner, the wide bandwidth will manifest itself as a low signal-to-noise ratio and resolution. However, it implies that the circuit does not necessarily need to be tuned to 600 MHz, as the coil will pick up signal from a range of frequencies about its peak.

B₁ Field Uniformity

A prototype of the Helmholtz coil design that used mechanically tunable capacitors was put into a 14-T MRI scanner to view the uniformity of the magnetic field. Images of various planes of a water-filled capillary were taken, using a 3D spin-echo sequence. Figure 8 describes the exact details of the sequence used to obtain the images below.

The most notable feature in Figure 9 is the meniscus. With the parameters of the spin-echo sequence, the meniscus came out very well and clear; however, it poses a problem in assessing the uniformity of the B_1 magnetic field of the Helmholtz coil. Figure 10 shows the signal intensity as a function of distance along the red line in Figure 9. Approaching the center of the coil, signal intensity increases, as is predicted by the simulations. Note that the scale is much larger than that of the MathCAD simulation. However, because of the meniscus, there is no water on the other side of the coil to assess whether or not the magnetic field created the “hourglass” shape that was predicted. There is a steep drop in intensity once the water stops. Therefore, the results of this particular scan are inconclusive in this respect and another scan should be done with a more carefully designed capillary.

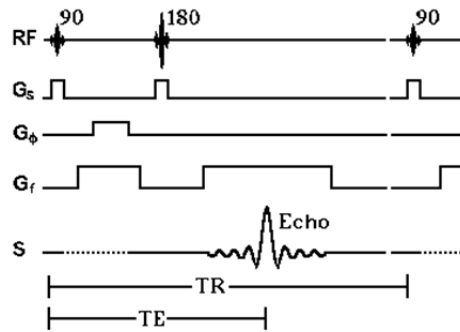


Figure 8: The field-of-view was $5 \times 3 \times 3$ mm and the data matrix was $166 \times 100 \times 100$; therefore, the voxel size was $0.0301 \times 0.03 \times 0.03$ mm. In the spin echo sequence, the repetition time, T_r was 1 s and the echo time, T_e , was 15 ms. The 90 degree pulse lasted $300 \mu\text{s}$ at 15.5 dB and the 180 degree pulse lasted $600 \mu\text{s}$ at 15.5 dB. Total scan time was approximately 11 hours. (Adapted from “The Basics of MRI” by Joseph Hornak³)

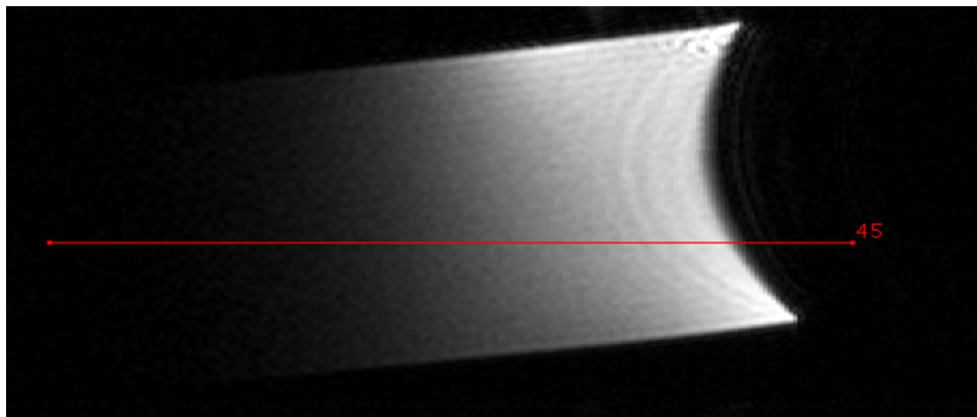


Figure 9: A meniscus is visible and clearly resolved, but it is a problem in assessing the uniformity of the B_1 magnetic field.

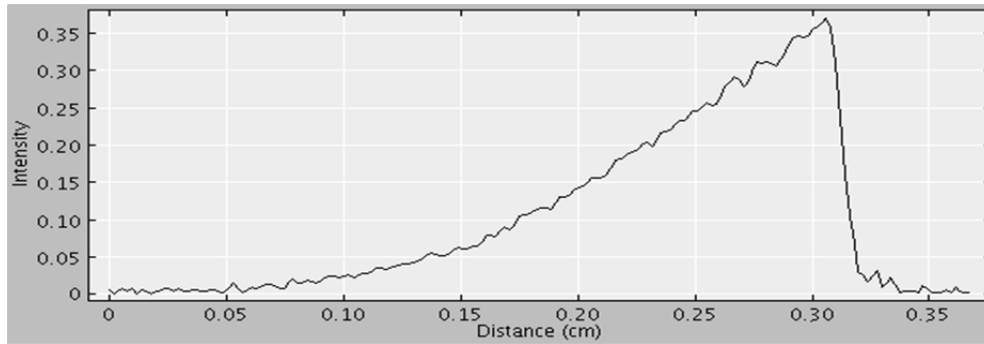


Figure 10: A graph of normalized intensity versus position begins similar to that predicted by models, but the meniscus causes a steep drop in intensity, which makes it impossible to see whether there is actually an “hour-glass” shape in the intensity of the magnetic field. Further scanning must be done.

A peculiarity visible in a different plane, shown in Figure 11, is a dark spot appearing towards the bottom right of the image. This is most likely due to the design flaw that the two Helmholtz loops are not complete circles. Using copper trace and two sides of a substrate, it is impossible to have two complete loops, as the trace must go through the board and continue on the other side so assure the circuit does not short. Besides the dark spot, the field passing through the midplane of the Helmholtz coil appears to be very uniform.

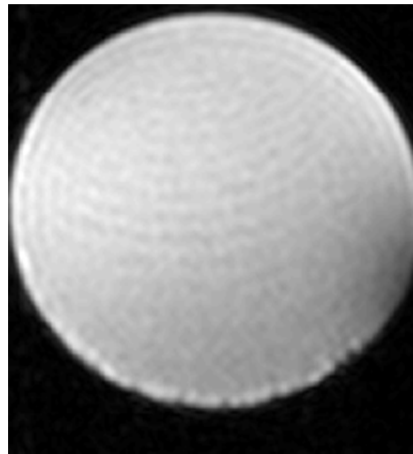


Figure 11: A dark spot appears in the bottom-right section of this image. This is probably due to the design of a copper-trace Helmholtz coil on a substrate. The coil is not a full 360 degrees, which causes a weakness in the B_1 field at the location of the gap.

Some of the images (not shown) contained artifacts. It is unclear at this point in time what was causing those artifacts, whether it was a design flaw of the coil, material on the outside of the capillary, or the sudden jump in intensity at the point of the meniscus. However, further testing can be done on various subjects to better assess the validity and usefulness of the current design.

DISCUSSION

As predicted, the Q factor of the varactors proved to be a limitation of their feasibility in tuning the resonance circuit. Though they seemed to be useful from the S_{11} sweep, they were not very useful according to the S_{21} sweep. The Q factor is inversely proportional with the frequency of the resonator, which means they are even less useful for MRI magnets stronger than 14 T.

However, the results of this study lead to numerous possible future projects. One such experiment would be to have the entire varactor setup, minus the

varactors. Replacing them with mechanical capacitors would and measuring S_{21} would prove if the extra traces and components are actually affecting the signal. The potential bias across the varactor may be interfering with the signal, which would mean that larger resistors must be used. If this is not the case, varactors may be unusable because the extra traces and components required add too much coupling to the circuit. Likewise, some of the signal may be lost through the entire loop created by the circuit on the substrate. Due to the lack of real-estate, the whole trace may be acting as its own inductor and lose some of the signal. This phenomenon was experienced to a small extent in the S_{21} parameter, though it was clear that the Helmholtz coil emitted most of the signal.

Another branch from the results of this study would be to experiment with different forms of digital tuning methods. A corollary to the Aeroflex Inc. hyperabrupt varactors used in this study would be high- Q abrupt-junction nonmagnetic varactors sold by companies, such as Cobham plc. Another possible component is a single-layer capacitor. Furthermore, it may actually be the silver paint used to bond the varactors to the trace that caused the issues at such a high frequency. This substance should be individually assessed to understand its properties at high frequency.

Future work may also include changing the Helmholtz coil design. With thicker materials, a successful Helmholtz coil with a 1.5-mm radius may be achievable. However, it may also be possible to wind thin wire to create a volume coil. The advantages of a wire-coil is that it would be very interchangeable, thus making interchangeable coils for various frequencies and it would be a round wire, as opposed to a flat trace where a magnetic field may not be created as uniformly. Due to the x - y grid that the laser etcher moves on, it had difficulty cutting a smooth arc on with such a small radius, leaving the edge of the trace jagged. The disadvantage of interchangeable coils is that they would not be physically as sturdy as a copper-trace coil fixed to a ceramic board. It is unclear whether this form of coil will reduce or augment the observation of artifact.

CONCLUSION

From the results gathered, it appears that images can be produced with varactors, but the signal-to-noise ratio of varactor-tuned circuits is not high enough to produce satisfying results for outside researchers looking to scan cells and other small objects. The varactor-tuned circuit can undergo more refinement to possibly produce better results, but the low Q of these components at high frequencies is a major pitfall. They do not have a very sharp S_{21} peak, which is indicative of the need for a change in either design or components. The Helmholtz coil showed the uniformity distribution predicted by the equations in MathCAD. This shows how the Helmholtz design is very sensitive to geometry and should be reconstructed more carefully.

Overall, using 10-pF isolating capacitors, 2-to-9-pF varactors, 1-M Ω resistors, and a 1.5-mm radius Helmholtz coil, a circuit can be tuned and impedance can be matched so that the circuit will resonate at 600 MHz when connected to a 50- Ω

coaxial cable. This is a useful result in the sense that it has pushed the learning curve of working with high frequency resonators, expanded a database for troubleshooting, and pointed future work in directions that will be more successful and closer to commercial transfer. Some potential applications of this research in the technological environment include the ability to study flow, diffusion, and perfusion of chemicals in real time, improved signal-to-noise ratio to understand structures of microscopic tissues, and alternative methods for finely tuning antennas.

ACKNOWLEDGMENTS

M. Feldman would like to thank Jeff Long and Amanda Baker for their knowledge and generosity with equipment that supported the project. Also, he would like to thank Haolun Zhang for his theoretical model and help in CST Microwave Studio. Lastly, he would like to thank Thomas Neuberger for his contribution in using the 14-T machine to scan a phantom. This material is based upon work supported by the National Science Foundation under Grant No. EEC-1062984.

REFERENCES

- [1] Weber, H., N. Baxan, D. Paul, J. Maclaren, D. Schmidig, M. Mohammadzadeh, J. Hennig, and D. Von Elverfeldt. "Microcoil-based MRI: Feasibility Study and Cell Culture Applications Using a Conventional Animal System." *Magnetic Resonance Materials in Physics, Biology and Medicine* 24.3 (2011): 137-45.
- [2] Haines, Kristina Noel. *Applications of High Dielectric Materials in High Field Magnetic Resonance*. Dissertation. The Pennsylvania State University, 2010.
- [3] Hornak, Joseph P. *The Basics of MRI*. Henrietta, NY: Interactive Learning Software, 1996. Web. <<http://www.cis.rit.edu/htbooks/mri/>>.